

1
2
3 **pH-responsive endosomolytic pseudo-peptides for drug delivery to multicellular**
4 **spheroids tumour models**
5
6

7 Vincent H.B. Ho^a, Nigel K.H. Slater^a, Rongjun Chen^{b,*}
8
9

10
11
12 ^a *Department of Chemical Engineering and Biotechnology, University of Cambridge,*
13
14 *New Museums Site, Pembroke St, Cambridge CB2 3RA, UK*
15

16
17 ^b *Centre for Molecular Nanoscience, School of Chemistry, University of Leeds, Leeds*
18
19 *LS2 9JT, UK*
20
21
22
23
24
25
26
27
28
29
30

31 * Corresponding author: Rongjun Chen,
32

33
34 E-mail: R.Chen@leeds.ac.uk
35

36 Telephone: +44 1133 439 102;
37

38
39 Fax: +44 1133 436 452
40
41
42
43
44
45
46
47
48
49
50
51
52
53
54
55
56
57
58
59
60
61
62
63
64
65

Abstract

1
2 Endosomolytic polymers can aid in the endosomal release of therapeutics to improve
3
4 intracellular drug delivery. pH-responsive biomimetic pseudo-peptides were
5
6 synthesised by grafting L-phenylalanine onto the pendant carboxylic acids of a
7
8 polyamide, poly(L-lysine isophthalamide). PP-75 (stoichiometric L-phenylalanine
9
10 grafting of 75 mol%) was determined to have the best endosomolytic property. The
11
12 mean hydrodynamic size of PP-75 decreased with lower pH as the polymers adopted
13
14 a more compact conformation due to protonation of acidic groups and increase in
15
16 hydrophobicity. PP-75 was demonstrated to deliver model drugs effectively in three
17
18 dimensional (3D) magnetic HeLa multicellular spheroids used as *in vitro* tumour
19
20 models. These spheroids can be isolated easily and quickly by magnetic separation.
21
22 Due to its relatively small size, PP-75 was able to penetrate from the exterior to the
23
24 interior of these spheroids and was internalised by the cells in the spheroids. It could
25
26 retain its pH-mediated membrane-lytic capability in 3D drug delivery by releasing
27
28 internalised calcein from intracellular endosomes in the tumour models. Furthermore,
29
30 cell viability results suggest that PP-75 showed no significant cytotoxicity towards
31
32 cells in the spheroids. The pH-responsive PP-75 can potentially enhance the
33
34 extracellular and intracellular delivery of therapeutics in tumours.
35
36
37
38
39
40
41
42
43
44
45

46 **Keywords:** drug delivery; pH-responsive polymer; L-phenylalanine; pseudo-peptide;
47
48 multicellular spheroids; magnetic separation
49
50
51
52
53
54
55
56
57
58
59
60
61
62
63
64
65

1. Introduction

1
2 One of the main aims of drug delivery research is the efficient intracellular
3 delivery of therapeutics, particularly macrodrugs such as proteins and nucleic acids.
4
5 Mammalian cells usually internalise macromolecular prodrugs through endocytosis
6
7 which results in endosomal localisation. After cellular uptake, internalised drugs face
8
9 several obstacles such as lysosomal degradation before they can reach their target
10
11 organelles or cell nuclei [1]. To prevent lysosomal degradation, drugs entrapped in
12
13 endosomes must be able to ‘escape’ into the cytosol before the endosomes fuse with
14
15 lysosomes. One strategy for endosomal release is through membrane disruption using
16
17 pH-responsive polymers [2]. These polymers can undergo pH-mediated coil-globule
18
19 changes in conformation and this property enhances their membrane disruptive
20
21 behaviour [3-7].
22
23
24
25
26
27

28
29 A class of biodegradable, pH-responsive polymers has been recently
30 developed to mimic factors that enable efficient viral transfection. The parent polymer
31 is a polyamide, poly(L-lysine isophthalamide), and hydrophobic amino acids were
32 grafted onto its pendant carboxylic acid groups to manipulate its amphiphilicity and
33 structure [8, 9]. Recent studies indicated that L-phenylalanine grafted polymers have
34 vastly superior membrane-disruptive activity at endosomal pHs and could be used for
35 intracellular drug delivery [10, 11].
36
37
38
39
40
41
42
43
44
45

46 Another important aspect of drug delivery is the transport of drugs through
47 extracellular barriers before they reach the cell surface. Penetration of
48 chemotherapeutics is often a problem for efficacious cancer therapy [12]. Ideally, the
49 drug should reach all cells in a tumour after leaving the vasculature. However, high
50 interstitial pressure within tumours [13], diffusion limitations and the extracellular
51 matrix [14] present significant obstacles to effective drug delivery. Therefore
52
53
54
55
56
57
58
59
60
61
62
63
64
65

1 relatively high drug concentrations were frequently used to overcome these problems.
2 This inevitably led to toxic side effects in patients [15].
3

4 Drug delivery systems serve to reduce the systemic toxicity by enhancing the
5 delivery of therapeutics to specific diseased sites at a lower dose. However these
6 systems are often studied using two dimensional (2D) cell monolayers which cannot
7 reproduce the complex three dimensional (3D) environment in tissues or organs. To
8 better model the actual *in vivo* conditions, 3D multicellular spheroids were developed
9 and they have been used as avascular tumour models for evaluating small molecule
10 [16] or nanoparticle [17, 18] delivery. Magnetic multicellular spheroids could be
11 generated from magnetically labelled cells. These spheroids can be easily separated
12 using magnetic separators and could be useful for various applications such as drug
13 screening and toxicity assays [19-21].
14
15
16
17
18
19
20
21
22
23
24
25
26
27

28 In this study, the relationship between pH and hydrodynamic size of L-
29 phenylalanine grafted polymers was examined. Furthermore, the potential of using
30 these grafted polymers for drug delivery in 3D magnetic tumour spheroids was
31 qualitatively and quantitatively assessed using confocal microscopy and flow
32 cytometry respectively. The non-specific cytotoxicity of the polymers towards cells in
33 the multicellular spheroids was evaluated as well.
34
35
36
37
38
39
40
41
42
43
44

45 **2. Materials and methods**

46 *2.1. Materials*

47 *2.1.1. Materials for polymer synthesis*

48 Isophthaloyl chloride, fluorescein 5-isothiocyanate (FITC), *N,N'*-
49 dicyclohexylcarbodiimide (DCC), 4-dimethylaminopyridine (DMAP), *N,N'*-
50 dimethylformamide (DMF), potassium carbonate and triethylamine were purchased
51
52
53
54
55
56
57
58
59
60
61
62
63
64
65

1 from Sigma-Aldrich (Dorset, UK). L-lysine methyl ester dihydrochloride and dimethyl
2 sulfoxide (DMSO) were obtained from Fisher (Loughborough, UK). L-phenylalanine
3 methyl ester hydrochloride was purchased from Alfa Aesar (Heysham, UK).
4
5
6
7
8
9

10 2.1.2. Materials for cell culture and drug delivery studies

11 Accutase[®], biotinamidohexanoic acid N-hydroxysuccinimide ester (BiotinSE),
12 calcein, Dulbecco's modified Eagle medium (DMEM), Dulbecco's phosphate
13 buffered saline (D-PBS), penicillin-streptomycin solution (10,000 U mL⁻¹ penicillin,
14 10 mg mL⁻¹ streptomycin) and trypsin-EDTA solution (0.5 g L⁻¹ porcine trypsin and
15 0.2 g L⁻¹ EDTA·4Na) were purchased from Sigma-Aldrich (Dorset, UK). Streptavidin
16 MagneSpheres paramagnetic particles (1 mg mL⁻¹) were purchased from Promega
17 (Southampton, UK). Foetal bovine serum (FBS) and propidium iodide (Invitrogen
18 P3566, 1 mg mL⁻¹) were purchased from Invitrogen (Paisley, UK).
19
20
21
22
23
24
25
26
27
28
29
30
31
32
33

34 2.2. Polymer synthesis and characterisation

35 PP-75 was synthesised by grafting L-phenylalanine onto poly(L-lysine
36 isophthalamide) according to the previously reported procedure [8, 10, 22-24] using
37 DCC as a coupling agent and DMAP as a hyperacylation catalyst [25, 26]. Here, the
38 number denotes the stoichiometric molar percentage of L-phenylalanine relative to the
39 pendant carboxylic acid groups of poly(L-lysine isophthalamide) ([NH₂]/[COOH]).
40 FTIR spectra of poly(L-lysine isophthalamide) and PP-75 were recorded on a Nicolet
41 Nexus FTIR spectrometer (Thermo Fisher Scientific, USA). FTIR (acid form): 3294
42 cm⁻¹ (N-H str and O-H str), 1720 cm⁻¹ (C=O acid str), 1634 cm⁻¹ (amide band I),
43 1528 cm⁻¹ (amide band II), 1274, 1088 cm⁻¹ (C-O str). The molecular weight and
44 polydispersity of poly(L-lysine isophthalamide) (M_w = 35,700, polydispersity = 1.99)
45
46
47
48
49
50
51
52
53
54
55
56
57
58
59
60
61
62
63
64
65

1 were determined using an aqueous gel permeation chromatography (GPC) system
2 (Viscotek, UK), which was calibrated with polyethylene glycol standards. ¹H-NMR
3 spectra of poly(L-lysine isophthalamide) and its derivative polymer PP-75 were
4 obtained in d₆-DMSO on a Bruker Advance 500 MHz NMR spectrometer (Bruker
5 Biospin GmbH, Germany). The degree of L-phenylalanine grafting of PP-75 (63.2
6 mol%) was measured from its ¹H-NMR spectrum, and used to calculate its molecular
7 weight ($M_n = 24.9$ kDa).
8
9

10
11
12
13
14
15
16
17
18
19
20
21
22
23
24
25
26
27
28
29
30
31
32
33
34
35
36
37
38
39
40
41
42
43
44
45
46
47
48
49
50
51
52
53
54
55
56
57
58
59
60
61
62
63
64
65
FITC-NH-(CH₂)₂-NH₂ was prepared from reaction of FITC with ethylene
diamine using dibutyltin dilaurate as a catalyst. The fluorescent polymer PP-75-FITC
(1 mol% FITC) was prepared by coupling FITC-NH-(CH₂)₂-NH₂ to the carboxylic
acid groups of PP-75 using standard DCC/DMAP mediated coupling techniques [10].

2.3. *Dynamic light scattering*

The hydrodynamic diameters of PP-75 were investigated using a
PDDLS/Batch dynamic light scattering (DLS) platform equipped with a PD2000DLS
detector (Precision Detectors, USA). The polymer aqueous solutions at 5 mg mL⁻¹
were prepared in 0.1 M buffers at specific pHs and allowed to equilibrate for 48 h.
The samples were filtered through 0.45 μm pore size filters, and then the
measurements were conducted in a 1.0 mL quartz cuvette using a diode laser of 800
nm at a scattering angle of 90°.

2.4. *Spheroid culture*

HeLa human cervix adenocarcinoma cells were cultured in DMEM
supplemented with 10% FBS, 100 U mL⁻¹ penicillin and 100 μg mL⁻¹ streptomycin
and maintained in a 5% CO₂ humidified atmosphere at 37°C. Magnetically labelled

1 HeLa cells were prepared using a previously developed method [27]. Briefly, HeLa
2 cells were treated with 750 μM BiotinSE in D-PBS at room temperature for 30 min.
3
4 0.05 mg mL^{-1} streptavidin paramagnetic particles were added to biotinylated HeLa
5 cells and vortexed for 15 s to ensure mixing of particles and cells. To generate
6 magnetic spheroids [19], 15 μL drops containing 500 magnetically labelled HeLa
7 cells each were added onto a culture dish cover lid. The lids were then inverted and
8 placed on top of the dish. 10 mL of PBS was added to prevent evaporation of the
9 hanging drops which were cultured in a 5% CO_2 humidified atmosphere at 37°C. Six
10 day old spheroids were harvested for further studies as described below.
11
12
13
14
15
16
17
18
19
20
21
22
23

24 *2.5. 3D drug delivery to spheroids*

25
26 For the concentration-dependent studies using PP-75-FITC, HeLa spheroids
27 were treated with different PP-75-FITC concentrations in serum-free DMEM for 1 h
28 at 37°C. For the time-dependent studies, HeLa spheroids were treated with 1 mg mL^{-1}
29 PP-75-FITC for different durations. PP-75-FITC was then removed and the spheroids
30 were washed with D-PBS and complete DMEM was added. The spheroids were then
31 further incubated at 37°C for 3.5 h before they were analysed using either confocal
32 microscopy or flow cytometry as depicted below.
33
34
35
36
37
38
39
40
41
42

43 For the study using calcein as a model drug, HeLa spheroids were treated with
44 different calcein concentrations with or without PP-75 (1 mg mL^{-1}) in serum-free
45 DMEM for 1 h at 37°C. Thereafter the spheroids were further incubated for 3.5 h at
46 37°C in complete DMEM before they were analysed using either confocal
47 microscopy or flow cytometry.
48
49
50
51
52
53
54
55
56
57

58 *2.6. Confocal laser scanning microscopy*

59
60
61
62
63
64
65

1 After the spheroids were treated according to the protocol described above,
2 they were placed on 35 mm glass-bottom culture dishes (MatTek) and imaged using a
3 Leica SP5 confocal laser scanning microscope. Both the PP-75-FITC and calcein
4 were excited using the 488 nm laser line. Optical sections (1 μm thick) were imaged
5 until the fluorescence was lost. These images were then compiled into a 3D
6 projection.
7
8
9
10
11
12
13
14
15
16

17 *2.7. Flow cytometry*

18
19 40–50 six day old HeLa spheroids were used for each experimental condition
20 as described above. Thereafter HeLa spheroids were separated using a Dynal MPC-S
21 magnetic particle concentrator (Invitrogen). After D-PBS wash, the spheroids were
22 enzymatically dissociated with Accutase[®]. The dissociated individual cells were
23 further washed with D-PBS and resuspended in D-PBS with 2.5 $\mu\text{g mL}^{-1}$ propidium
24 iodide. The cells were then analysed by flow cytometry (BD FACSCan). 10,000
25 events were recorded and the data was analysed using CellQuest. FITC fluorescence
26 intensities of 20 arbitrary units (a.u.) and above were regarded as FITC-positive (+),
27 as the control sample recorded fluorescence intensities of less than 20 a.u. Cell
28 viability was assessed by gating cell populations showing negligible propidium iodide
29 fluorescence.
30
31
32
33
34
35
36
37
38
39
40
41
42
43
44
45
46
47
48
49

50 **3. Results and discussion**

51 The hydrodynamic size of PP-75 was measured using DLS and it showed a pH
52 dependent size change. At pH 6.0, PP-75 has a mean hydrodynamic diameter of 17
53 nm (Fig. 1a). The hydrodynamic size increases as the pH increases with a mean
54 diameter of 37 nm at the physiological pH of 7.4, as shown in Fig. 1b. This pH
55
56
57
58
59
60
61
62
63
64
65

1 dependent behaviour occurred as PP-75 alters its conformation according to pH
2 changes. The hydrophobicity of the polymer increases as the pH decreases with the
3
4 protonation of free carboxylic acid groups and growing hydrophobic interactions
5
6 between the grafted L-phenylalanine, resulting in an even more compact structure [8].
7
8

9
10 PP-75, the L-phenylalanine grafted polymer with the most promising property
11 for endosomal membrane disruption [10], was selected for 3D delivery studies in
12 magnetic HeLa tumour spheroids. PP-75 labelled with fluorescein 5-isothiocyanate
13 (PP-75-FITC) was incubated with magnetic HeLa multicellular spheroids and
14 confocal microscopy was used to study the distribution of the fluorescent polymer in
15 the spheroids. Fig. 2 shows that the 3D delivery of PP-75-FITC is dependent on both
16 polymer concentration and incubation duration. More polymers can be delivered into
17 the spheroids when there is a higher polymer concentration or longer incubation time,
18 as shown by the stronger fluorescence. The images in the Y-Z axis show that the
19 polymers were able to penetrate into the spheroids.
20
21
22
23
24
25
26
27
28
29
30
31
32
33

34 The use of confocal microscopy to visualise polymer penetration into the
35 spheroids suffers from an imaging depth limitation due to the loss of fluorescent
36 signal and increased background at depths greater than 100–200 μm [28]. To
37 overcome this constraint and to obtain a more quantitative analysis, flow cytometry
38 was used for further studies. HeLa spheroids which have been treated with PP-75-
39 FITC were enzymatically dissociated into individual cells and the cells were then
40 analysed using a flow cytometer.
41
42
43
44
45
46
47
48
49
50

51 Quantitative data in Fig. 3 further proved that the 3D delivery of PP-75, shown
52 as the proportion of FITC positive cells and mean FITC fluorescence intensity of the
53 cell population, is dependent on both the polymer concentration and incubation
54 duration with the polymer. Compared to HeLa cells grown as a monolayer, higher
55
56
57
58
59
60
61
62
63
64
65

1
2
3
4
5
6
7
8
9
10
11
12
13
14
15
16
17
18
19
20
21
22
23
24
25
26
27
28
29
30
31
32
33
polymer concentrations were needed to achieve a significant distribution in the HeLa
spheroids. When HeLa cell monolayers were treated with 0.05 mg mL⁻¹ of PP-75-
FITC for 1 h, 74% of cells had taken up the fluorescent polymer. With increasing
polymer concentration to 0.1 mg mL⁻¹, almost all monolayer cells (97%) were FITC-
positive. As comparison, treatment with 0.05 mg mL⁻¹ of PP-75-FITC for 1 h only
achieved 19% cellular uptake of the polymer in HeLa spheroids. The proportion of
FITC-positive cells was saturated at 93% with increasing polymer concentration up to
5 mg mL⁻¹ (Fig. 3a). When the incubation duration with PP-75-FITC (1 mg mL⁻¹) was
extended from 15 min to 2 h, the proportion of FITC-positive cells in the spheroids
increased gradually from 34% to 83% (Fig. 3 c). There is less difficulty with diffusion
for cell monolayers, while the delivery of polymers into the spheroids faced diffusion
limitations and additional barriers such as the extracellular matrix [14]. Therefore
higher polymer concentrations are required for efficient delivery in spheroids. This is
likely the same situation for effective polymer delivery *in vivo*.

34
35
36
37
38
39
40
41
42
43
44
45
46
47
48
49
50
51
52
53
54
55
56
57
58
59
60
61
62
63
64
65
Cell viability in the multicellular spheroids was analysed by flow cytometry
using the propidium iodide exclusion assay to evaluate the non-specific cytotoxicity
of PP-75-FITC towards the cells in the spheroids. Propidium iodide can enter non-
viable cells with permeable membranes and binds with intracellular nucleic acids by
intercalation. As shown in Fig. 4a, the polymer was not drastically toxic to HeLa cells
at concentration up to 4 mg mL⁻¹ after 1 h of treatment. Fig. 4b shows that PP-75-
FITC (1 mg mL⁻¹) only had a relatively low level of cytotoxic effect with extended
incubation time to 2 h. These results suggest that PP-75 will probably have a similar
toxicity profile, since the degree of FITC labelling (1 mol%) is kept low to avoid
significant modulation of the polymer properties and fluorescence quenching [10].

1 To study whether PP-75 still retains its membrane-lytic activity in 3D
2 delivery, magnetic HeLa spheroids were treated with free calcein (as a model drug)
3 and PP-75. Calcein, which has been internalised by cells, is trapped within endosomes
4 and undergo self-quenching with reduced fluorescence when excited with lasers. This
5 quenching effect could be reduced when calcein is released from the endosomes and
6 is freely dispersed within the cytoplasm [29].
7
8
9
10
11
12
13

14 The confocal images (Fig. 5c, d) showed that more calcein was released from
15 endosomes when PP-75 was co-incubated with it. Flow cytometric analysis further
16 confirmed that PP-75 was able to help attain higher intracellular calcein fluorescence
17 within the spheroids (Fig. 6). What is even more significant is that PP-75 (with 2 mg
18 mL⁻¹ calcein) was able to achieve higher calcein fluorescence compared to the 4 mg
19 mL⁻¹ free calcein control. This could mean that lower drug concentrations can be used
20 in polymer-mediated delivery. Non-specific cytotoxicity and side effects of drugs
21 could then be minimised.
22
23
24
25
26
27
28
29
30
31
32
33

34 In the study above, PP-75 was able to penetrate efficiently into the 3D
35 multicellular spheroids and achieve a reasonable concentration in the spheroids (Fig. 2
36 and 3). When the polymers were internalised, they were able to disrupt endosomal
37 membranes for effective intracellular release of endocytosed calcein (Fig. 5 and 6).
38 The transport of PP-75 in the spheroids might be less obstructed due to its small size
39 (Fig. 1), which makes it easier to diffuse through the extracellular space. Studies have
40 shown that penetration of nanoparticles into the core of multicellular spheroids was
41 limited to particles smaller than 100 nm [17, 18]. It was demonstrated that adeno-
42 associated viral vectors (~25 nm in diameter) can penetrate human solid tumour tissue
43 *in vivo* more efficiently than adenoviral vectors (~100 nm in diameter) [30], which
44 could be attributed at least in part to these differences in particle size. In addition,
45
46
47
48
49
50
51
52
53
54
55
56
57
58
59
60
61
62
63
64
65

grafting with the hydrophobic amino acid L-phenylalanine can facilitate effective cell surface binding, which is necessary for uptake of the polymer.

Fig. 1 shows that PP-75 formed a compact structure (37 nm in diameter at pH 7.4) stabilised by hydrophobic association. The mean hydrodynamic diameters of these polymeric nanoparticles gradually reduced to 17 nm with pH decreasing to 6.0. It is known that *in vivo* tumours have lower extracellular pH than normal tissues [31]. Moreover, pH gradients exist within spheroids and tumours with the pH decreasing from the exterior to the interior [32]. As PP-75 migrated through the spheroids, it experienced decreasing pH and could undergo further size reduction. This could have actually aided in the penetration of PP-75 towards the core of the multicellular spheroids and resulted in a higher proportion of cells which internalised the polymer.

This work represents the first time that magnetic multicellular spheroids were used as tumour models in drug delivery research. These spheroids can be easily separated using a magnetic separator within a few seconds without the need for centrifugation. This allows for facile separation of spheroids after incubation with drugs or drug delivery systems for further examination using other analytical techniques such as confocal microscopy and flow cytometry used in this study. As mentioned previously, the magnetic property of these spheroids will make them suitable for large scale or high throughput studies requiring large amounts of spheroids and quick separation for subsequent investigations [19]. Furthermore, recent studies also showed that 3D multicellular spheroids have great potential for predicting *in vivo* experimental results in drug delivery [33].

4. Conclusions

1
2
3
4
5
6
7
8
9
10
11
12
13
14
15
16
17
18
19
20
21
22
23
24
25
26
27
28
29
30
31
32
33
34
35
36
37
38
39
40
41
42
43
44
45
46
47
48
49
50
51
52
53
54
55
56
57
58
59
60
61
62
63
64
65

In this current study, it was shown that the pH-responsive, biodegradable and biomimetic polymers grafted with L-phenylalanine have significant potential to be used to deliver therapeutics. In particular, the endosomolytic polymer, PP-75 (63.2 mol% L-phenylalanine, $M_n = 24.9$ kDa), shows a pH-dependent change in its hydrodynamic size. The effective penetration of PP-75 into tumour models and its ability to release internalised model drugs within cells in tumour spheroids suggest that it could be studied in *in vivo* or clinical research to further evaluate and realise its potential for delivering therapeutics to tumours.

Acknowledgements

Vincent Ho would like to thank the Agency for Science, Technology and Research (Singapore) for a National Science Scholarship (PhD). Rongjun Chen wishes to thank the Biomedical and Health Research Centre (Leeds, United Kingdom) for the Senior Translational Research Fellowship. The authors would like to thank Biotechnology and Biological Sciences Research Council (United Kingdom) for financial support.

References

1. Ganta S, Devalapally H, Shahiwala A, Amiji M. A review of stimuli-responsive nanocarriers for drug and gene delivery. *J Control Release* 2008;126(3):187-204.
2. Murthy N, Robichaud JR, Tirrell DA, Stayton PS, Hoffman AS. The design and synthesis of polymers for eukaryotic membrane disruption. *J Control Release* 1999;61(1-2):137-143.
3. Tonge SR, Tighe BJ. Responsive hydrophobically associating polymers: a review of structure and properties. *Adv Drug Deliv Rev* 2001;53(1):109-122.
4. Yessine MA, Leroux JC. Membrane-destabilizing polyanions: interaction with lipid bilayers and endosomal escape of biomacromolecules. *Adv Drug Deliv Rev* 2004;56(7):999-1021.
5. Liechty WB, Kryscio DR, Slaughter BV, Peppas NA. Polymers for drug delivery systems. *Annu Rev Chem Biomol Eng, Vol 1* 2010;1:149-173.
6. Lin YL, Jiang G, Birrell LK, El-Sayed ME. Degradable, pH-sensitive, membrane-destabilizing, comb-like polymers for intracellular delivery of nucleic acids. *Biomaterials* 2010;31(27):7150-7166.
7. Ding H, Inoue S, Ljubimov AV, Patil R, Portilla-Arias J, Hu J, et al. Inhibition of brain tumor growth by intravenous poly(beta-L-malic acid) nanobioconjugate with pH-dependent drug release. *Proc Natl Acad Sci U S A* 2010;107(42):18143-18148.
8. Chen R, Eccleston ME, Yue Z, Slater NKH. Synthesis and pH-responsive properties of pseudo-peptides containing hydrophobic amino acid grafts. *J Mater Chem* 2009;19(24):4217-4224.
9. Chen R, Khormae S, Eccleston ME, Slater NK. Effect of L-leucine graft content on aqueous solution behavior and membrane-lytic activity of a pH-responsive pseudopeptide. *Biomacromolecules* 2009;10(9):2601-2608.
10. Chen R, Khormae S, Eccleston ME, Slater NK. The role of hydrophobic amino acid grafts in the enhancement of membrane-disruptive activity of pH-responsive pseudo-peptides. *Biomaterials* 2009;30(10):1954-1961.
11. Liechty WB, Chen R, Farzaneh F, Tavassoli M, Slater NK. Synthetic pH-responsive polymers for protein transduction. *Adv Mater* 2009;21(38-39):3910-3914.
12. Minchinton AI, Tannock IF. Drug penetration in solid tumours. *Nat Rev Cancer* 2006;6(8):583-592.
13. Boucher Y, Baxter LT, Jain RK. Interstitial pressure gradients in tissue-isolated and subcutaneous tumors: implications for therapy. *Cancer Res* 1990;50(15):4478-4484.

- 1
2
3
4
5
6
7
8
9
10
11
12
13
14
15
16
17
18
19
20
21
22
23
24
25
26
27
28
29
30
31
32
33
34
35
36
37
38
39
40
41
42
43
44
45
46
47
48
49
50
51
52
53
54
55
56
57
58
59
60
61
62
63
64
65
14. Netti PA, Berk DA, Swartz MA, Grodzinsky AJ, Jain RK. Role of extracellular matrix assembly in interstitial transport in solid tumors. *Cancer Res* 2000;60(9):2497-2503.
15. Brannon-Peppas L, Blanchette JO. Nanoparticle and targeted systems for cancer therapy. *Adv Drug Deliv Rev* 2004;56(11):1649-1659.
16. Bryce NS, Zhang JZ, Whan RM, Yamamoto N, Hambley TW. Accumulation of an anthraquinone and its platinum complexes in cancer cell spheroids: the effect of charge on drug distribution in solid tumour models. *Chem Commun* 2009(19):2673-2675.
17. Goodman TT, Ng CP, Pun SH. 3-D tissue culture systems for the evaluation and optimization of nanoparticle-based drug carriers. *Bioconj Chem* 2008;19(10):1951-1959.
18. Goodman TT, Olive PL, Pun SH. Increased nanoparticle penetration in collagenase-treated multicellular spheroids. *Int J Nanomedicine* 2007;2(2):265-274.
19. Ho VH, Muller KH, Barcza A, Chen R, Slater NK. Generation and manipulation of magnetic multicellular spheroids. *Biomaterials* 2010;31(11):3095-3102.
20. Friedrich J, Ebner R, Kunz-Schughart LA. Experimental anti-tumor therapy in 3-D: spheroids--old hat or new challenge? *Int J Radiat Biol* 2007;83(11-12):849-871.
21. Lee J, Lilly GD, Doty RC, Podsiadlo P, Kotov NA. In vitro toxicity testing of nanoparticles in 3D cell culture. *Small* 2009;5(10):1213-1221.
22. Eccleston ME, Slater NKH, Tighe BJ. Synthetic routes to responsive polymers; co-polycondensation of tri-functional amino acids with diacylchlorides. *React Funct Polym* 1999;42(2):147-161.
23. Eccleston ME, Kuiper M, Gilchrist FM, Slater NK. pH-responsive pseudo-peptides for cell membrane disruption. *J Control Release* 2000;69(2):297-307.
24. Eccleston ME, Slater NKH, inventors. Hypercoiling polymers and their use in cellular delivery. Patent No. WO2004052402, EP1567194 (A1), US2006172418 (A1), AU2003290222 (A1); 2004.
25. Haslam E. Recent developments in methods for the esterification and protection of the carboxyl group. *Tetrahedron* 1980;36(17):2409-2433.
26. Okada Y. Synthesis of peptides by solution methods. *Curr Org Chem* 2001;5(1):1-43.
27. Ho VH, Barcza A, Chen R, Muller KH, Darton NJ, Slater NK. The precise control of cell labelling with streptavidin paramagnetic particles. *Biomaterials* 2009;30(33):6548-6555.

- 1
2
3
4
5
6
7
8
9
10
11
12
13
14
15
16
17
18
19
20
21
22
23
24
25
26
27
28
29
30
31
32
33
34
35
36
37
38
39
40
41
42
43
44
45
46
47
48
49
50
51
52
53
54
55
56
57
58
59
60
61
62
63
64
65
28. Wartenberg M, Hescheler J, Acker H, Diedershagen H, Sauer H. Doxorubicin distribution in multicellular prostate cancer spheroids evaluated by confocal laser scanning microscopy and the "optical probe technique". *Cytometry* 1998;31(2):137-145.
 29. Jones RA, Cheung CY, Black FE, Zia JK, Stayton PS, Hoffman AS, et al. Poly(2-alkylacrylic acid) polymers deliver molecules to the cytosol by pH-sensitive disruption of endosomal vesicles. *Biochem J* 2003;372(Pt 1):65-75.
 30. Enger PO, Thorsen F, Lonning PE, Bjerkvig R, Hoover F. Adeno-associated viral vectors penetrate human solid tumor tissue in vivo more effectively than adenoviral vectors. *Hum Gene Ther* 2002;13(9):1115-1125.
 31. Danhier F, Feron O, Preat V. To exploit the tumor microenvironment: passive and active tumor targeting of nanocarriers for anti-cancer drug delivery. *J Control Release* 2010;148(2):135-146.
 32. Sutherland RM. Cell and environment interactions in tumor microregions: the multicell spheroid model. *Science* 1988;240(4849):177-184.
 33. Kim TH, Mount CW, Gombotz WR, Pun SH. The delivery of doxorubicin to 3-D multicellular spheroids and tumors in a murine xenograft model using tumor-penetrating triblock polymeric micelles. *Biomaterials* 2010;31(28):7386-7397.

Figure Captions

Figure 1. Mean hydrodynamic diameters of PP-75 at 5 mg mL⁻¹ in 0.1 M buffers. (a) Size distribution at pH 6.0. (b) pH-dependent mean hydrodynamic diameters. Error bars represent standard deviations of four samples.

Figure 2. Confocal microscopy images of HeLa spheroids treated with PP-75-FITC at (a, b) 0.05 mg mL⁻¹ for 1 h, (c, d) 4 mg mL⁻¹ for 1 h, (e, f) 1 mg mL⁻¹ for 2 min and (g, h) 1 mg mL⁻¹ for 2 h. Samples were imaged after 3.5 h further incubation. (a, c, e, g) show the image in the X-Y axis, while (b, d, f, h) show the image in the Y-Z axis.

Figure 3. Flow cytometric analysis of cellular uptake of PP-75-FITC in HeLa multicellular spheroids. (a, b) Concentration-dependent uptake of PP-75-FITC after treatment for 1 h. (c, d) Time-dependent uptake of PP-75-FITC at 1 mg mL⁻¹. Samples were tested after 3.5 h further incubation. (a, c) show the proportion of FITC-positive cells, while (b, d) show the relative mean fluorescence intensity (MFI) of cell population expressed in arbitrary units (a.u.). Relative MFI = (MFI_{sample}/MFI_{control}). 40-50 spheroids were used for each experimental condition and the spheroids were enzymatically dissociated for subsequent flow cytometric analysis.

Figure 4. Concentration- and time-dependent cell viabilities of HeLa spheroids treated with PP-75-FITC. (a) PP-75-FITC concentration-dependent studies. Spheroids were treated with various concentrations of PP-75-FITC for 1 h with 3.5 h further incubation in fresh complete culture media. (b) PP-75-FITC treatment duration-dependent studies. Spheroids were treated with 1 mg mL⁻¹ PP-75-FITC for various durations with 3.5 h further incubation in fresh complete culture media. Relative cell viabilities were expressed in percentage based on the control without polymer treatment. 40-50 spheroids were used for each experimental condition and the spheroids were enzymatically dissociated for subsequent flow cytometric analysis using the propidium iodide exclusion assay.

Figure 5. Confocal microscopy images of HeLa spheroids treated with (a, b) 2 mg mL⁻¹ calcein for 1 h, and (c, d) 2 mg mL⁻¹ calcein with 1 mg mL⁻¹ PP-75 for 1 h. Samples were imaged after 3.5 h further incubation. (a, c) show the image in the X-Y axis, while (b, d) show the image in the Y-Z axis.

Figure 6. Flow cytometric analysis of cellular uptake of calcein and PP-75 in HeLa spheroids. Spheroids were treated with various concentrations of calcein with or without PP-75. Samples were tested after 3.5

h further incubation. Relative mean fluorescence intensity (MFI) of cell population was expressed in arbitrary units (a.u.). Relative MFI = $(MFI_{\text{sample}}/MFI_{\text{control}})$. 40-50 spheroids were used for each experimental condition and the spheroids were enzymatically dissociated for subsequent flow cytometric analysis.

Figure 1

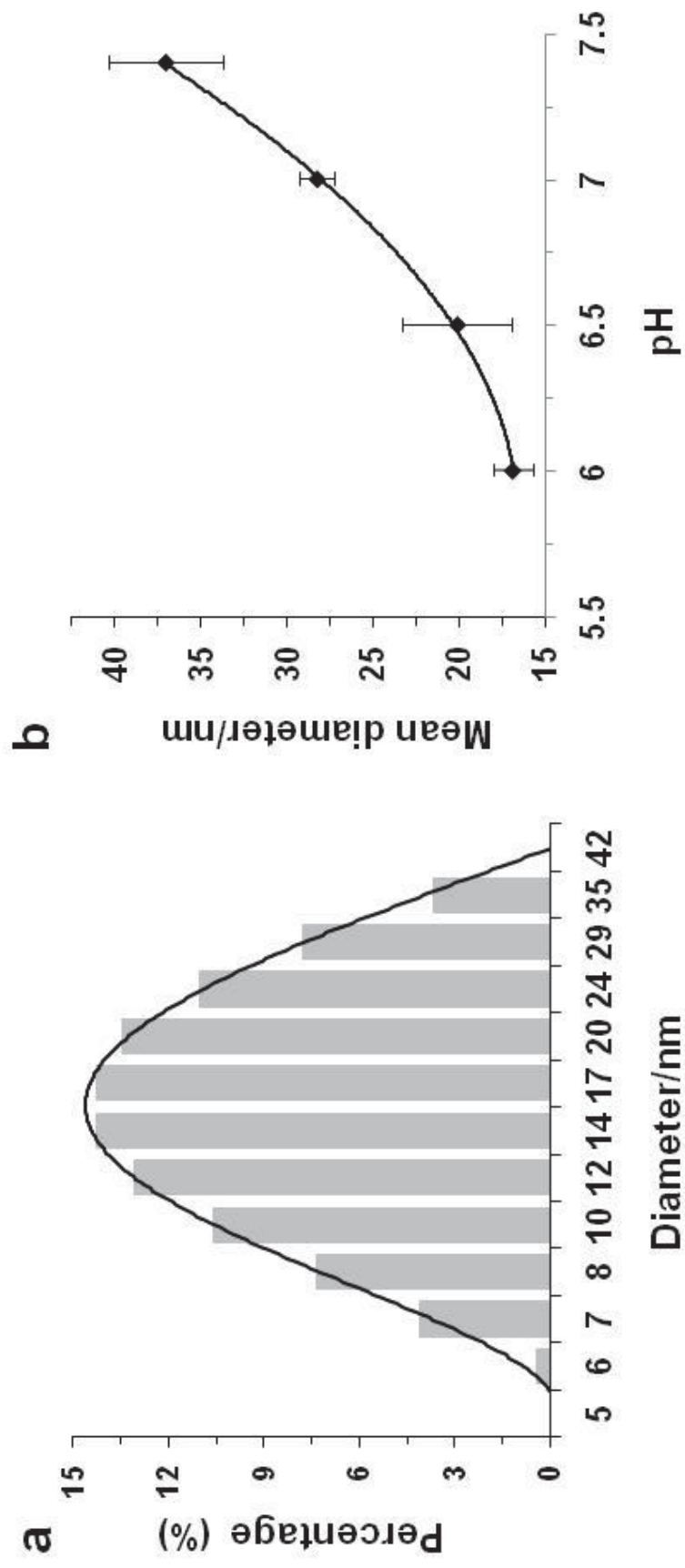


Figure 2

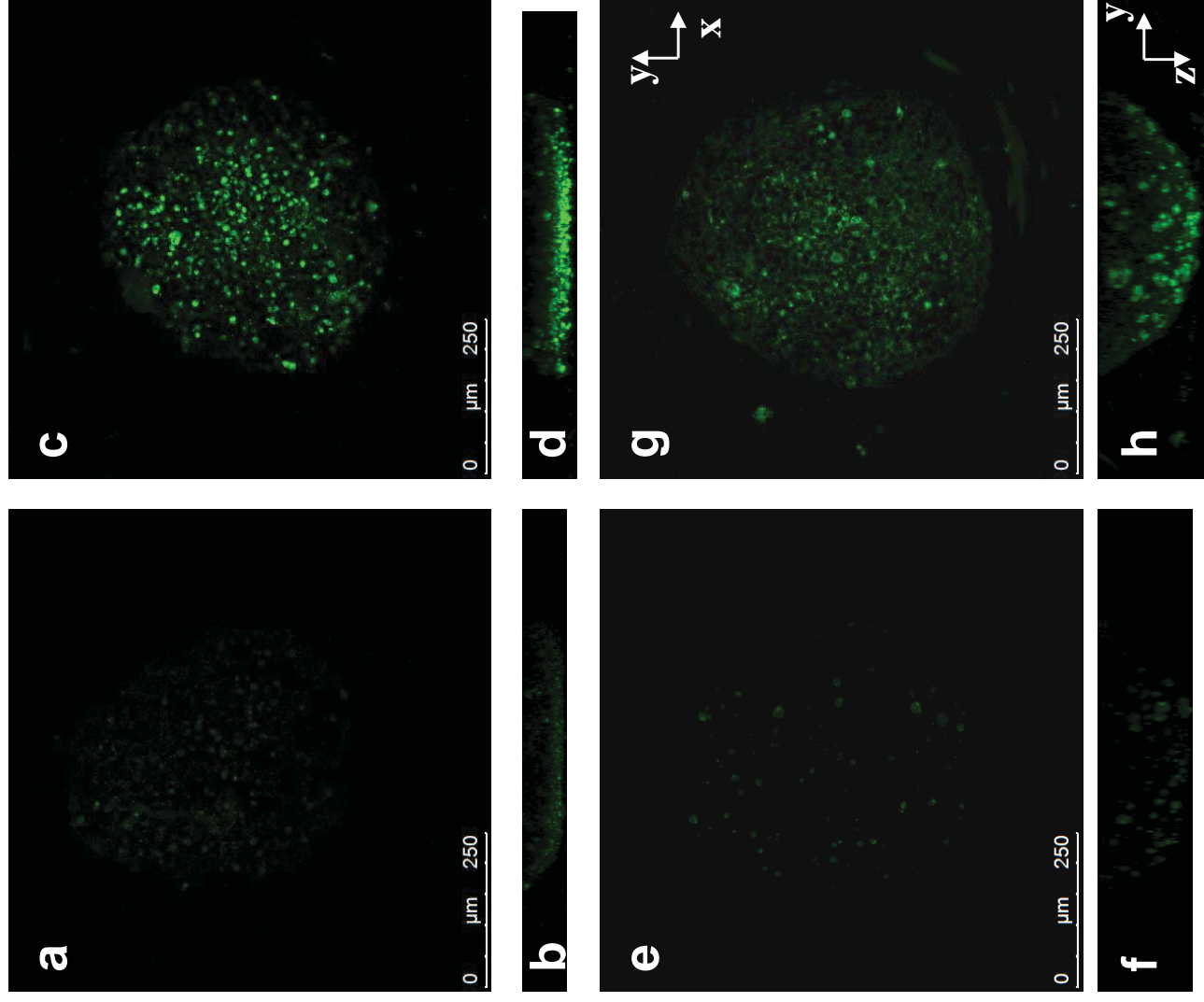


Figure 3

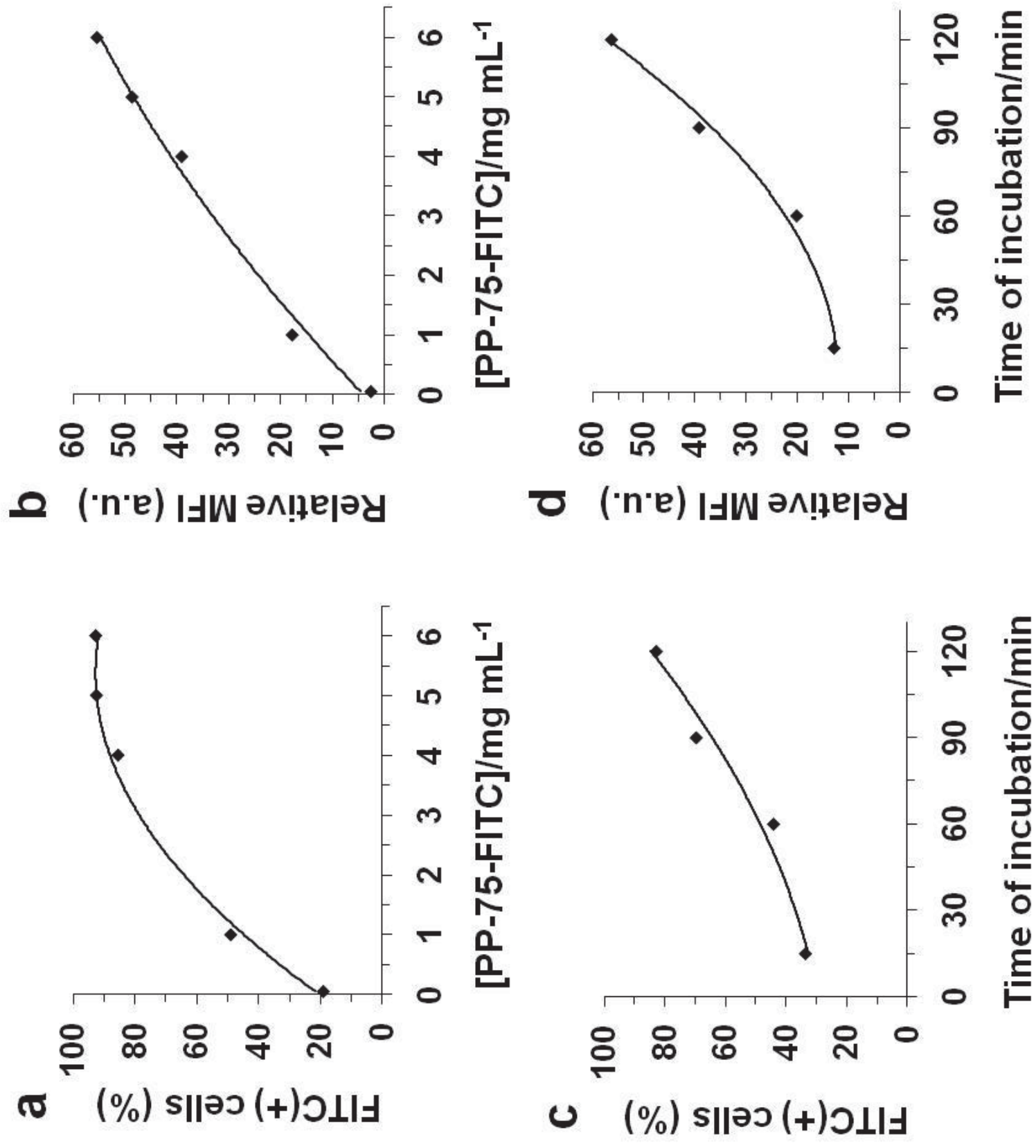


Figure 4

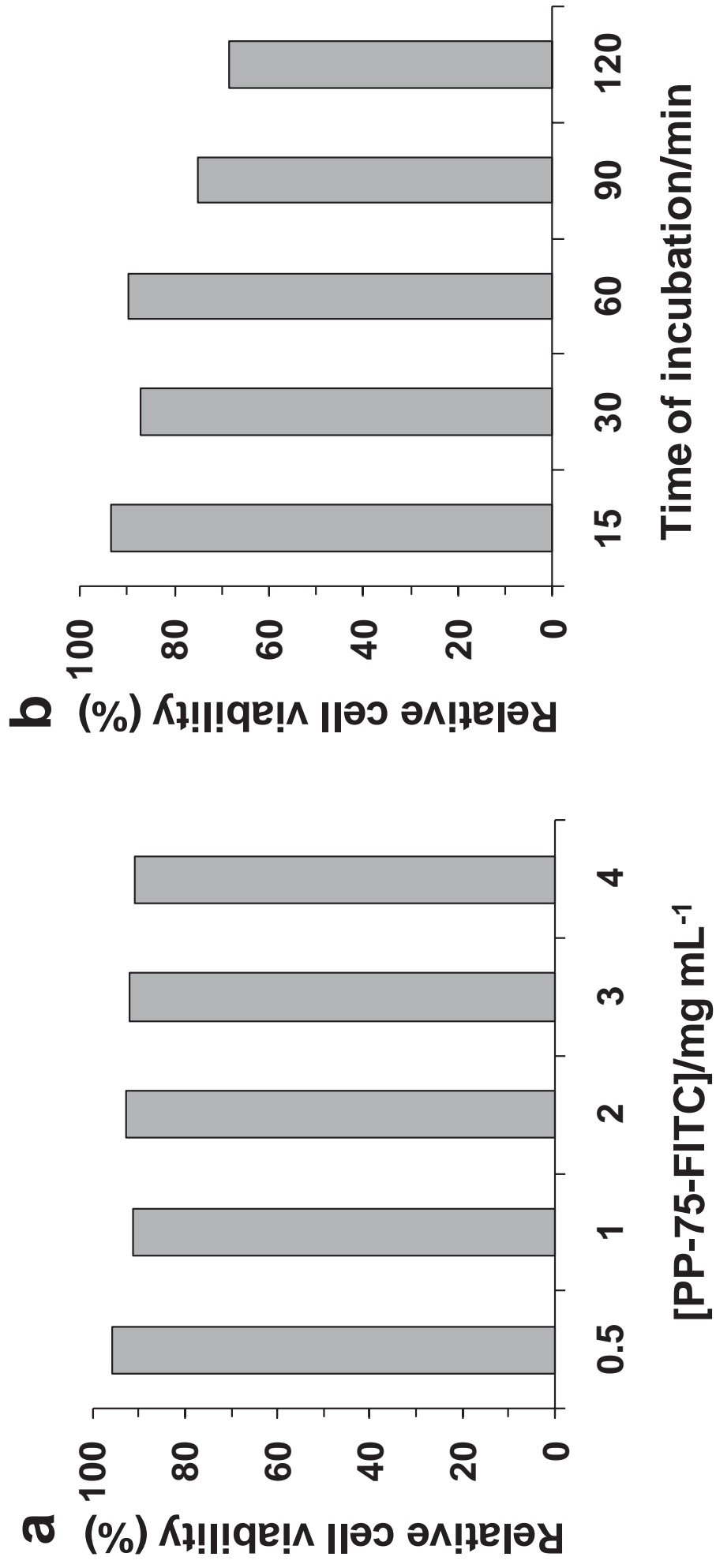


Figure 5

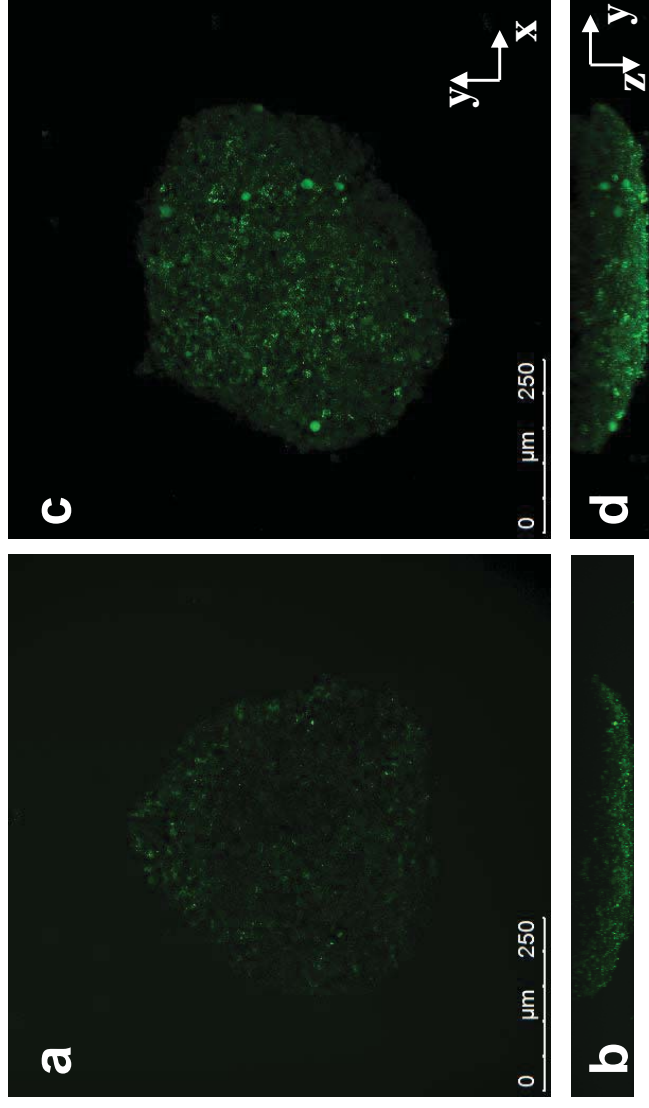
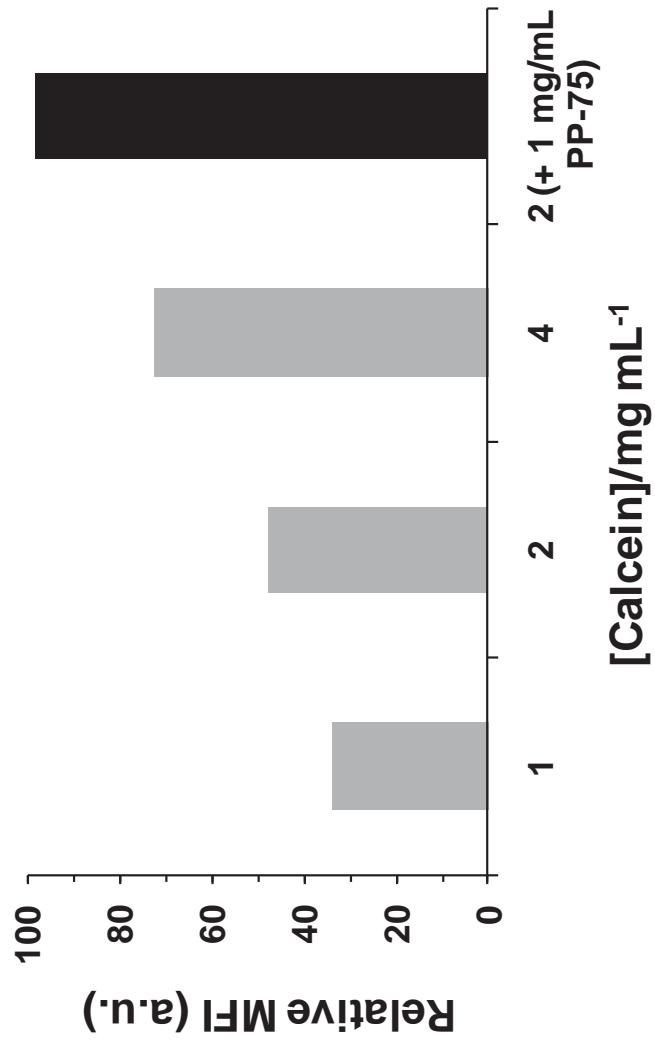


Figure 6



Supplementary Data

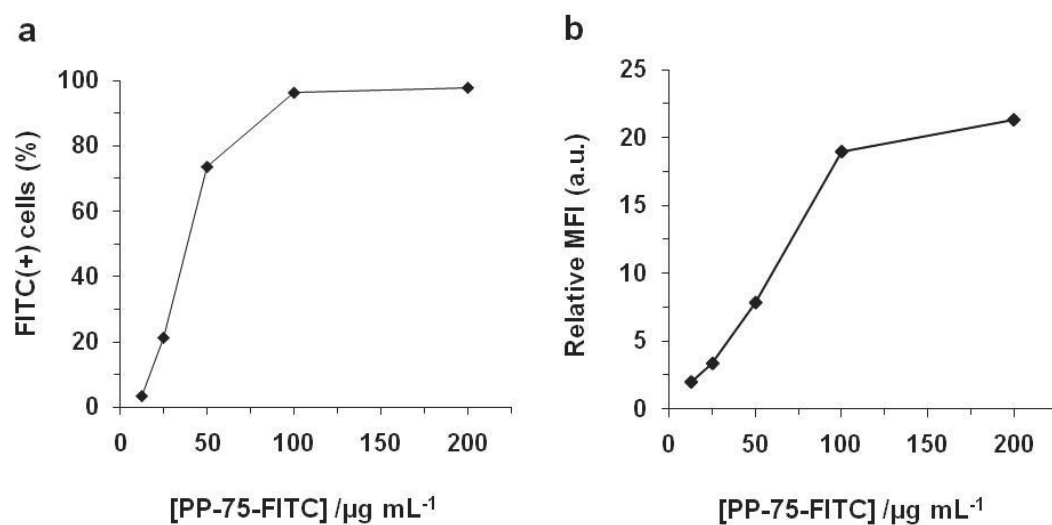


Fig. S1 Flow cytometric analysis of cellular uptake of PP-75-FITC in HeLa cell monolayers. Samples were treated with PP-75-FITC for 1 h and tested after 3.5 h further incubation. (a) Proportion of FITC-positive cells. (b) Relative mean fluorescence intensity (MFI) of cell population expressed in arbitrary units (a.u.). Relative MFI = $(\text{MFI}_{\text{sample}}/\text{MFI}_{\text{control}})$.